Parametric Optimization of Dye-Sensitized Solar Cells Using Far red Sensitizing Dye with Cobalt Electrolyte

著者	Pradhan A, Saikiran M, Kapil G, Pandey S S., Hayase S
journal or publication title	Journal of Physics: Conference Series
volume	924
number	1
page range	012001-1-012001-9
year	2017-11
URL	http://hdl.handle.net/10228/00006528

doi: https://doi.org/10.1088/1742-6596/924/1/012001

Parametric Optimization of Dye-Sensitized Solar Cells Using Far red Sensitizing Dye with Cobalt Electrolyte

IOP Conf. Series: Journal of Physics: Conf. Series **924** (2017) 012001 doi:10.1088/1742-6596/924/1/012001

Parametric Optimization of Dye-Sensitized Solar Cells Using Far red Sensitizing Dye with Cobalt Electrolyte

A Pradhan*, M Saikiran, G Kapil, S S. Pandey* and S Hayase

Graduate School of LSSE, Kyushu Institute of Technology, 2-4, Hibikino, Wakamatsu, Kitakyushu 808-0196, Japan
E-mail: ansupradhan9@gmail.com;shyam@life.kyutech.ac.jp

Abstract. A far-red sensitizing dye **SQ-75** has been employed as a model sensitizer with $Co(bpy)^{2+/3+}$ redox electrolytes to fabricate dye-sensitized solar cells (DSSCs) and optimize the various device parameters which influence the overall photoconversion efficiency (PCE). It has been found that the optimization of the TiO_2 thickness, surface treatment with $TiCl_4$, and an optimum amount of the chenodeoxycholic acid (CDCA) as coadsorber are necessary to attain the overall improved PCE. $TiCl_4$ surface treatment on both FTO and TiO_2 has been found to outperform as compared to their untreated counterparts owing to the suppression of the charge recombination. DSSCs with an optimized TiO_2 thickness of 6 μm and CDCA concentration of 4 mM have exhibited best performance due to enhanced photon harvesting and reduced dye aggregation, respectively.

1. Introduction

Dye-sensitized solar cells (DSSCs) have been emerged as one of the potential candidates amongst next generation solar cells owing to their low production cost, ease of fabrication and widely tunable optical properties [1]. DSSC is basically a photoelectrochemical cell which is typically comprised of a sensitizing dye adsorbed to the surface of wide band gap semiconductor like TiO_2 as a photoanode, Platinum (Pt) coated conducting substrate as a photocathode and an electrolyte system containing redox couple [2-4]. The dyes which are heart of this kind of solar cells plays a crucial role in photon harvesting since they actually absorb the sun light and controls the overall obtainable photoconversion efficiency (PCE) and have shown nearly quantitative photon harvesting in the visible wavelength region [5-7]. In order to enhance the PCE even higher, there has been a continuous research in developing the sensitizing dyes having photon harvesting in the far-red to near infra-red (NIR) wavelength region a various dyes including dyes from squaraine family have attempted to extend the light absorption as well as photon harvesting in the red to NIR spectral region [8-15]. Recent past has witnessed that DSSCs have successfully achieved a PCE of 11.9% with iodine (I_3^-/ I^-) based electrolytes [15] even having efficient photon harvesting mainly in the visible region of the solar spectrum only. However, disadvantages such as potential loss, corrosion and competitive light absorption by iodine based redox electrolyte itself have limited the efficiency of DSSCs compelled the search for alternate redox electrolytes to circumvent these issues. In this context, new alternative redox mediators such as based on cobalt complexes redox

shuttles have been successfully employed to achieve higher open circuit voltage (Voc) as well as high PCE [16-20]. Interestingly, a theoretical PCE reaching 20% with an assumption of minimal potential loss and better fill factor, can be attained by combining NIR and visible dye. Unfortunately there are no report regarding fabrication of DSSCs employing NIR dyes and cobalt complex based redox shuttles to be best of our knowledge. Therefore, we feel that squaraine dyes having sharp and intense light absorption mainly in the far-red to NIR region as a representative model of NIR dyes with Cobalt complex based electrolyte is an important and interesting area of research to be focused on and knowledge can be used for fabrication of high efficiency DSSCs.

Squaraine dyes exhibit narrow full width at half maximum and very high molar extinction coefficients and tunable light absorption form visible to IR wavelength region. They show strong dye aggregation behavior due to their relatively planar molecular structure and extended π–conjugation [10]. Therefore, we have accepted these challenges and tried to improve the efficiency of DSSCs based on squaraine dyes specially utilizing cobalt complex based redox electrolyte. A well-known dye de-aggregating agent chenodeoxycholic acid (CDCA) was co-adsorbed on the nanoporous TiO_2 surface along with the dye molecules to prevent dye aggregation [21]. In this work, we have employed an unsymmetrical squaraine dye (SQ-75) as a representative of NIR dye with $Co(bpy)^{2+/3+}$ redox electrolyte. Device fabrication parameters such as thickness of mesoporous TiO_2 layer, and surface treatment with $TiCl_4$ affects the performance of DSSCs [22-28], hence, similar kinds of experiments have also been carried out in current study on this novel dye-electrolyte combination in order to optimize the performance.

2. **Materials and methods**

Unsymmetrical squaraine dye SQ-75 and cobalt complex based redox electrolyte was synthesized following the methodology as per our earlier publications [9,29]. After the synthesis and purification by silica-gel column chromatography, structure of SQ-75 was confirmed by 1H nuclear magnetic resonance and fast ion bombardment-mass spectrometry. Electronic absorption spectra of the sensitizing squaraine dye (SQ-75) in ethanol solution as well as the dye adsorbed on thin films of the mesoporous TiO_2 was measured with a UV-visible-NIR spectrophotometer (JASCO, V670). DSSC fabrication was started with the cleaning of fluorine doped tin oxide (FTO) glasses by detergent solution, distilled water, acetone, isopropanol and acetone for 10 minutes each. After this, the photoanodes were prepared by screen-printing mesoporous DS/P and 30 NRD TiO_2 pastes (Solaronix) on FTO followed by baking at 500^0C for 30 min. This coating procedure was done one or several times to obtain TiO_2 thickness in the range of 2 to 18 μm especially for the thickness optimization of mesoporous TiO_2 layer. Some of the samples were pre and post-treated to freshly prepared TiO_2 films with aqueous $TiCl_4$ solution. This TiO2 surface treatment was conducted by dipping the substrates dipped in the 40 mM aqueous $TiCl_4$ solution at 80^0C for 30 min under continuous magnetic stirring at 500 rpm followed by the sintering at 500^0C for 30 minutes. Different photoanodes such as TiO_2 only (untreated samples), bottom $TiCl_4$ (pre-treated samples) on FTO, top $TiCl_4$ (post-treated samples) on mesoporous TiO2 and top/bottom $TiCl_4$ (pre and post-treated samples) were prepared for the current study. All of the samples were dipped in 0.2 mM dye solution in ethanol containing a fixed amount of CDCA varying from 2 mM to 30 mM for 4 hours at room temperature. For optimization of TiO_2 thickness and concentration of CDCA top/bottom $TiCl_4$ based photoanodes were taken. Counter electrode was prepared by FTO glass sputtered with 240 nm Ti followed 40 nm Pt and DSSC was assembled using this counter electrode with the photoanode and a 25 μm thick Himilan film (Mitsu-Dupont) spacer which melts at 110^0C by pressing the two parts for 20-30 seconds. Electrolyte was then injected and cell was finally sealed using UV resin to avoid any solvent leakage. The electrolyte was composed of 0.22 mM $Co(bpy)_3(PF_6)_2$, 0.033 mM $Co(bpy)_3(PF_6)_3$, 0.2 M tertiary butyl pyridine and 0.1 M $LiClO_4$ in Acetonitrile for all of the devices. Chemical structure of the unsymmetrical squaraine dye (SQ-75) and bipyridyl ligand bearing cobalt complex based redox electrolyte used in this work have been shown in the Fig.1

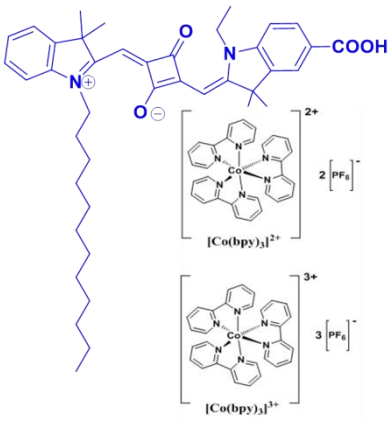

Figure 1. Molecular structure of sensitizing dye SQ-75 and cobalt complex based redox electrolyte.

Photovoltaic (PV) performances of the devices were measured with a solar simulator (CEP-2000, Bunko-Keiki, Japan) equipped with a xenon lamp (XLS-150A). The intensity of light irradiation was adjusted to AM 1.5 (100 mW/cm^2) using a spectroradiometer (LS-100, Eiko Seiki, Japan). The exposure power was also corrected with a standard amorphous Si photo detector (BS-520 S/N 007, Bunko-Keiki, Japan), which has similar light sensitivity to the DSSCs. Irradiation area of 0.2025 cm^2 was precisely controlled by a black metal mask for all of the samples during the measurement of photovoltaic characteristics. Incident photon to current conversion efficiency (IPCE) as a function of wavelength for the devices prepared were also measured with a constant photon flux of 1 x 10^{16} photon per cm^2 at each wavelength in the direct current mode using the action spectrum measurement system connected to the solar simulator.

3. Result and Discussion

3.1 Dye Design and Electronic Absorption Spectra

It has been found that molecular structure of dyes plays a crucial role to control the performance DSSCs especially using cobalt based redox electrolytes where dyes in general possess multiple and long alkyl chains [15, 20, 30]. This importance of alkyl chain for the sensitizers of DSSCs based on cobalt complex based electrolyte was further experimentally verified by the fact ruthenium based dye N-719 which works very well with iodine based electrolyte exhibit very poor performance with cobalt electrolyte. At the same time its long alkyl chain substituted analogue Z-907 works very well with cobalt based electrolytes [31]. Actually long alkyl chains of the dyes lead to effective surface passivation of the mesoporous TiO_2 surface and suppress the charge recombination by preventing obvious electrostatic attractive interaction between the positively charged cobalt complex ions with the negatively charged TiO_2 surface [32]. Keeping this mind we logically selected the unsymmetrical squaraine dye SQ-75 having very long dodecyl substituent at the opposite end of the dye from the –COOH functionalized indole ring as anchoring site. This not only supports the facile dye anchoring but also effectively passivates the negatively charged TiO_2 surface.

Owing to the flat molecular structure of squaraine dyes which are prone to the easy dye aggregation, CDCA has been most widely used in combination with dye as coadsorber to prevent the dye aggregation [21, 33]. Electronic absorption spectra of the SQ-75 in ethanol solution in the presence as well as well as absence of CDCA along with in solid-state thin film adsorbed on TiO_2 are shown in Fig. 2. Electronic absorption spectrum of SQ-75 in ethanol solution (5 mM with 4 mM CDCA) exhibits a very sharp absorption peak having absorption maximum (λ_{max}) at 638 nm with very high molar extinction coefficient of 3.18 x 10^5 dm^3.mol^{-1}.cm^{-1} along with vibronic shoulder at 592 nm. This is a typical characteristic of squaraine dyes and this sharp electronic absorption peak is associated with the

π-π^* electronic transition [4, 10]. Interestingly in the absence of CDCA also neither there is any shift in the spectral shape nor position of the λ_{max} which indicates that at in solution state at this concentration there is no dye aggregation and dye exists in the monomeric form. Upon absorption on the mesoporous TiO_2 not only there is spectral broadening as compared to that observed in solution but also there is enhancement in the intensity of the vibronic shoulder. This spectral broadening is attributed to the interaction between TiO_2 and dye molecules in the condensed state as reported previously [28]. The small difference in the intensity of the vibronic shoulder in the presence as well as absence of CDCA on TiO_2 suggests that long alkyl chain present in the dye are also involved in the suppression of dye aggregation in the condensed state.

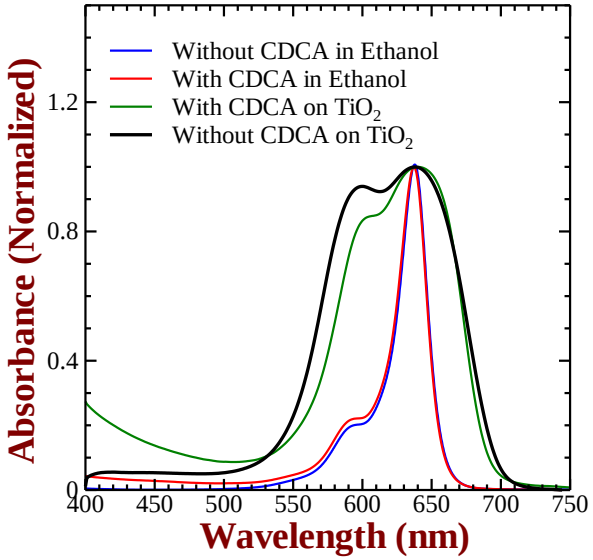

Figure 2. Electronic absorption spectra of SQ 75 ethanol solution and thin film adsorbed on mesoporous TiO_2 (3 μm).

3.2. Influence of $TiCl_4$ Surface Treatment

DSSCs have been fabricated in the device configuration of FTO/TiO_2/dye/Electrolyte/Pt with different interfaces between its all components and they are expected to work optimally for good device performances. Amongst these, FTO/TiO_2/dye interfaces play an important role in deciding the overall PCE [21-23]. Open circuit voltage (Voc) for a device varies inversely to the recombination rates at these interfaces, which in turn affects the short current density (Jsc) and fill factor (FF) also [24]. Control of this charge recombination by surface passivation using compact and conformal TiO_2 layer has been well documented. This surface passivation especially for DSSCs based on cobalt complex based electrolytes is more crucial owing to their relatively bulky nature as compared to iodine redox electrolyte counterparts and their relatively slow diffusion imparts more chances for the charge recombination [17]. Apart from passivation, the compact TiO_2 layer has been reported to play various roles such as to increase the TiO_2 surface area, to enhance electron transport, to promote light scattering and dye anchoring, which finally results in better device performance [22]. In this work, attempts have been made to investigate the role of this compact layer on overall device performance and to demonstrate that which one plays the predominant role. In order to predict this effect more explicitly, other factors such as thickness of mesoporous TiO_2 layer (6-7μm), dye (SQ-75), dye/CDCA ratio (1/50) and electrolyte $Co(bpy)^{2+/3+}$ were kept the same.

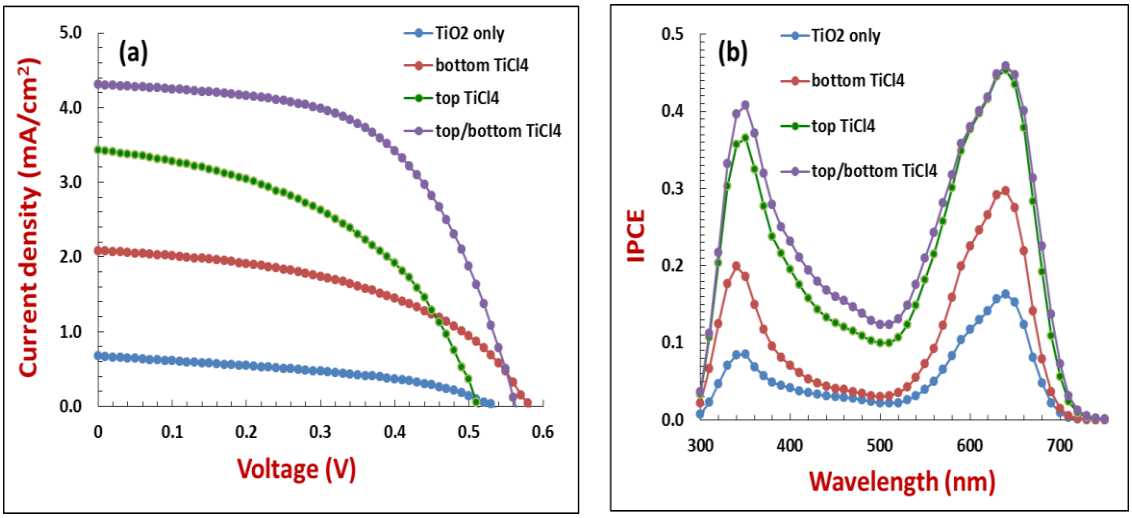

Figure 3. Photovoltaic characteristics of DSSCs under simulated solar irradiation (a) and photocurrent action spectra (b) after monochromatic incident light for DSSCs with different types of $TiCl_4$ surface treatments.

Figure 3(a) shows the current-voltage (I-V) characteristics of fabricated DSSCs under simulated solar condition of 1.5 AM with different surface treatment conditions. The short circuit current density (J_{sc}), open circuit voltage (V_{oc}), fill factor (FF) and the overall PCE (η) have been summarized in the Table 1. All of the DSSCs with $TiCl_4$ treatment exhibited better device performance as compared to that of untreated one due to reduced charge recombination. It can be clearly seen from this figure that surface treatment on mesoporous TiO_2 (top $TiCl_4$) has more pronounced effect than that on the FTO (bottom $TiCl_4$) which is concluded due to the rise in current density of 2.08 mA/cm^2 to 3.48 mA/cm^2 and hence the PCE of 0.57% to 0.81%. This increase in current density is well supported by the increased IPCE of 30% to 45 % between the wavelengths from 600-700 nm as shown in Fig 3(b). The beneficial effect of the $TiCl_4$ treatment is best presented by J_{sc} = 4.31 mA/cm^2, V_{oc} = 0.56 V, FF = 0.56 and η = 1.34%, when surface treatment was conducted on both of the FTO as well as mesoporous TiO_2 (top/bottom $TiCl_4$). IPCE shown in Fig. 3(b) also confirms the far-red photon harvesting by the sensitizer and maxima of the observed IPCE is in accordance with the Jsc measured in the I-V characteristics.

Table 1. Photovoltaic parameters for DSSC based on SQ-75 having $TiCl_4$ surface treatments conducted jon different surfaces of photoanode.

Treatment conditions	Jsc (mA/cm^2)	Voc (V)	FF	Efficiency (%)
No surface treatment	0.67	0.53	0.41	0.14
Treatment only on FTO	2.08	0.58	0.47	0.57
Treatment on TiO_2 only	3.43	0.51	0.46	0.81
Treatment on both TiO_2 and FTO both	4.31	0.56	0.56	1.34

3.3 Thickness of Mesoporous TiO_2 layer

Optimizing the thickness of light absorbing layer is an important issue to be solved as it affects the solar cell performance mainly the Jsc [26]. It can be easily understood that if the thickness of absorber layer is less, in that case most of the light transmits without proper absorption. Therefore, a minimum optimized thickness is must for proper device functioning. This

minimum thickness of the absorber layer will be less if the absorption coefficient of the absorbing material dyes is high. However, there is limitation on the maximum thickness of absorbing layer also, as with the increase in thickness after certain limit the chances of recombination increase because photoexcited electrons has to travel a long distance compared to their diffusion length [1]. This diffusion length varies for different dye and electrolyte systems used in DSSCs and need to be optimized for obtaining the better device functioning. In case of DSSCs, the absorbing layer thickness totally depends on mesoporous TiO_2 layer which acts as a scaffold for the dye monolayer. Hence, we can control and confirm the optimized thickness for better results by varying the thickness of mesoporous TiO_2 thickness.

In the present work, DSSCs were fabricated by varying the thickness of mesoporous TiO_2 layer in top/bottom $TiCl_4$ treated photoanodes keeping other variables such as dye concentration, electrolyte, CDCA concentration constant. Table 2 summarizes photovoltaic parameters obtained from I-V characteristics of the DSSCs. A perusal of table 2 corroborates the increase in thickness of the mesoporous TiO_2 layer from 2 μm to 4 μm there is increase in Jsc and PCE from 2.4 mA/cm^2 to 3.38 mA/cm^2 and 0.51% to 0.88%, respectively, due to enhanced photon harvesting. With further increase in the thickness of the mesoporous TiO_2 up to 6 μm, it was noticed that devices achieved their best Jsc of 5.33 mA/cm^2 and PCE of 1.43% whose photovoltaic characteristic is shown in the Fig. 4. When the thickness was increased more than 6 μm to 8 μm, there was a sharp decrease in the PCE as a function of thickness as shown in the inset of the Fig. 4. For Ruthenium complex based dyes (N-719) it has been demonstrated that 15 μm thick TiO_2 layer was optimum for achieving the best efficiency [26]. Therefore, we conclude that in our case, for the DSSC using sensitizing dye SQ-75 having a high molar extinction coefficient nearly 10 times as compared to typical ruthenium based sensitizers, a relatively thinner TiO_2 (6 μm) is capable of sufficient photons harvesting.

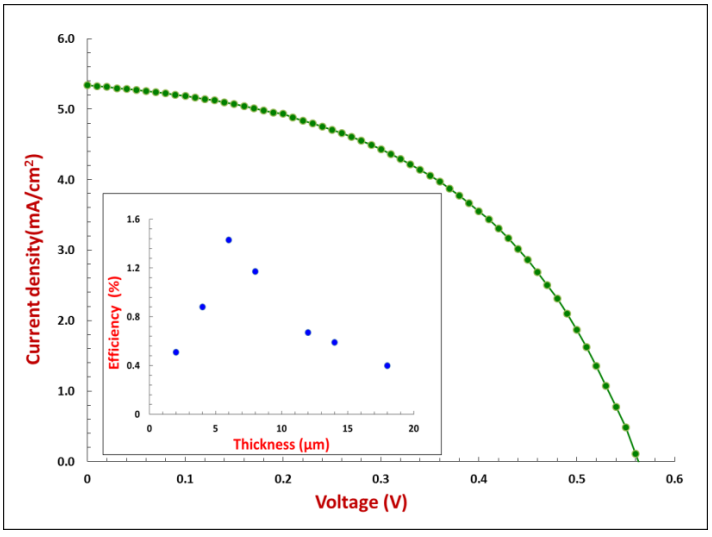

Figure 4. Photovoltaic characteristic of DSSC with TiO_2 layer thickness of 6 μm under simulated solar irradiation. Inset shows the thickness dependence of PCE.

Table 2. Photovoltaic characteristics of DSSC with varying thickness of mesoporous TiO_2.

Thickness	2 µm	4 µm	6 µm	8 µm	12 µm	14 µm	18 µm
Efficiency (%)	0.51	0.88	1.43	1.17	0.67	0.59	0.4
FF	0.37	0.47	0.48	0.55	0.47	0.5	0.48
V_{oc} (V)	0.56	0.55	0.56	0.56	0.55	0.55	0.52
J_{sc} (mA/cm^2)	2.4	3.378	5.33	3.75	2.59	2.1	1.62

3.4 Influence of CDCA Concentration

Squaraine dyes are prone to dye aggregate formation because of their planarity and extended π conjugation facilitated by the π-π stacking and lead to the hampered charge injection. Thus to prevent these dye aggregates, an adequate amount of CDCA has been most commonly used functions which not only functions as coadsorber but also suppresses the dye aggregation [21]. As CDCA plays the role of coadsorber without actually participating in photon harvesting, hence optimization for its adequate amount is necessary for the optimum device performance. For the optimization, top/bottom $TiCl_4$ based photoanode was implemented along with the same mesoporous TiO_2 thickness (6 µm), dye concentration and electrolyte. Figure 5 presents the plot of change in PCE for the DSSCs fabricated by changing the concentration of CDCA. Device containing 4 mM of CDCA in dye solution exhibited an improved PCE of 1.57% compared to the device without any CDCA (1.3%). Further increase in the CDCA concentration with respect to the dye resulted in to decrease of the PCE. This behavior could be understood considering the fact that presence of excess amount of CDCA inhibits the dye molecules present on the mesoporous TiO2 surface due to competitive adsorption and hampers the effective absorption of the incident photons. It is also interesting to note that SQ-75 dye structure is less prone to dye aggregation as devices without CDCA also showed the comparatively good PCE of 1.3% to that of the devices with CDCA as shown in Table 3.

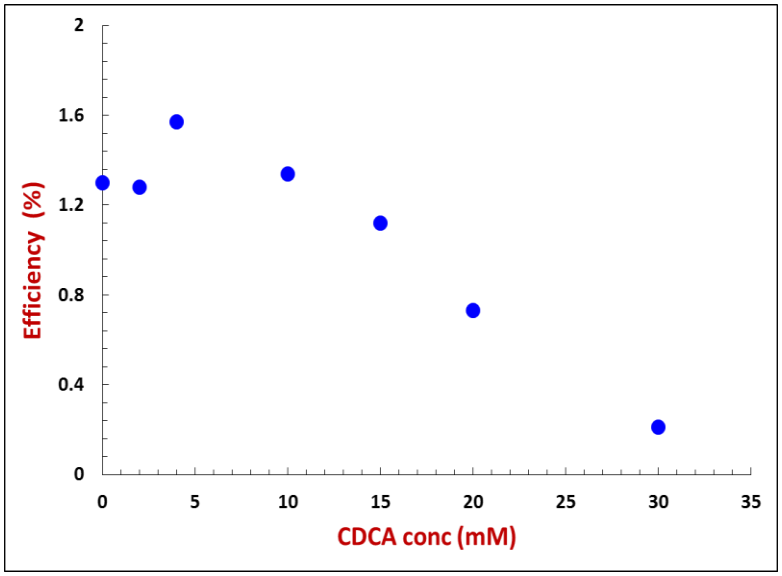

Figure 5. Effect of coadsorber CDCA concentration on the PCE of DSSCs based on SQ-75 and $Co(bpy)^{2+/3+}$ redox electrolyte.

*-***Table 3. Photovoltaic parameters for DSSCs with varying concentration of CDCA with SQ-75.

CDCA conc. (mM)	0	2	4	10	15	20	30
Efficiency (%)	1.3	1.28	1.57	1.34	1.12	0.73	0.21
Voc(V)	0.55	0.55	0.56	0.56	0.56	0.55	0.53
J_{sc} (mA/cm^2)	4.30	4.56	5.67	4.31	4.14	2.55	1.17
FF	0.55	0.51	0.49	0.56	0.48	0.49	0.35

4. Conclusions

In summary, optimization of DSSCs fabricated using a model unsymmetrical squaraine dye SQ-75 and $Co(bpy)^{2+/3+}$ redox electrolyte pertaining to the different device fabrication parameters have been amicably conducted in order to achieve the optimum PCE. $TiCl_4$ surface treatment was found to control the overall PCE and especially it was more effective when treatment was done on both of the FTO glass substrate and mesoporous TiO_2 layer leading to the best PCE of 1.34 %. It was also found that mesoporous TiO_2 thickness variation also affects the device performance and thickness of 6 μm was best suited for DSSCs based on this dye-electrolyte system. Finally, the PCE of SQ-75 dye based DSSCs seem to be less affected by the dye aggregation owing to its special molecular design as confirmed by photovoltaic measurements as well as electronic absorption spectral investigations.

Acknowledgments

One of the authors (SSP) would like express sincere thanks to Japan Society for the Promotion of Science (JSPS) for the financial support by Grant-in-Aid for Scientific Research (C) (Grant Number 26410206).

References:

[1] Grätzel M 2009 *Acc. Chem. Res.* **42** 1788
[2] Kakiage K, Aoyama Y, Yano T, Otsuka T, Kyomen T, Unno M and Hanaya M 2014 *Chem. Commun. 50 6379*
[3] Wang M, Grätzel C, Zakeeruddin S M, Grätzel M 2012 *Energy Environ. Sci.* **5** 9394
[4] T Morimoto, N Fujikawa, Y Ogomi, S S Pandey and S Hayase 2016 *Journal of Physics: Conference Series.* pp. 12002-12008.
[5] Ito S, Murakami T N, Comte P, Liska P, Grätzel C, Nazeeruddin M K, Grätzel M 2008 *Thin Solid Films* **516** 4613
[6] Gao F, Wang Y, Shi D, Zhang J, Wang M, Jing X, Humphry-Baker R, Wang P, Zakeeruddin S M, Grätzel M 2008 *J. Am. Chem. Soc.* **130** 10720
[7] Barbe C J, Arendse F, Comte P, Jirousek M, Lenzamann F, Shklover V, Grätzel M 1997 *J. Am. Ceram. Soc.* **80** 3157
[8] Sreejith S, Carol P, Chithra P, Ajayaghosh A 2008 *J. Mater. Chem.* **18** 264
[9] Pandey S S, Inoue T, Fujikawa N, Yamaguchi Y, Hayase S 2010 *Thin Solid Films.* **519** 1066
[10] Morimoto T, Fujikawa N, Ogomi Y, Pandey S S, Ma T, Hayase S 2016 *J. Nanosci. Nanotechnol.* (In press)
[11] J Chang, C P Lee, D Kumar, P W Chen, L Y Lin, K J Thomas and K C Ho 2013 *Journal of Power Sources*. **240** 779-785.
[12] Hara K, Tachibana Y, Ohga Y, Shinpo A, Suga S, Sayama K, Sugihara H, Arakawa H 2013 *Sol. Energy Mater. Sol. Cells* **77** 89
[13] C H Chang, Y C Chen, C Y Hsu, H H Chou and J T Lin 2012 *Organic letters*. **14** 4726-4729.
[14] F M Jradi, X Kang, D O'Neil, G Pajares, Y A Getmanenko, P Szymanski, T C Parker, M A El-Sayed and S R Marder 2015 *Chemistry of Materials*. **27** 2480-2487.
[15] Mathew S, Yella A, Gao P, Humphry-Baker R, Curchod BF, Ashari-Astani N, Tavernelli I, Rothlisberger U, Nazeeruddin M K, Gratzel M 2014 *Nat. Chem.* **6** 242
[16] Jihuai W, Zhang L, Jianming L, Miaoliang H, Yunfang H, Leqing F and Genggeng L 2015 *Chem.*

Rev. **115** 2136
[17] Zong X, liang M, Fan C, Tang K, Li G, Sun Z, Xue S 2012 *J. Phys. Chem. C*. **116** 11241
[18] M J DeVries, M J Pellin and J T Hupp 2010 *Langmuir*. **26** 9082-9087.
[19] M J Marchena, G de Miguel, B Cohen, J A Organero, S Pandey, S Hayase and A Douhal 2013 *The Journal of Physical Chemistry C*. **117** 11906-11919.
[20] S M Feldt, E A Gibson, E Gabrielsson, L Sun, G Boschloo and A Hagfeldt 2010 *Journal of the American Chemical Society*. **132** 16714-16724.
[21] J. H. Yum, S. J. Moon, R. H. Baker, P. Walter, T. Geiger, F. Nuesh, M. Grätzel, and M. K. Nazeeruddin, *Nanotechnology* 19, 424005(2008).
[22] Yoshida Y, Tokashiki S, Kubota K, Shiratuchi R, Yamaguchi Y, Kono M, Hayase S 2008 *Sol. Energy Mater. Sol. Cells* **92** 646
[23] Sommeling P M, O'Regan B C, Haswell R R, Smit H J P, Bakker N. J, Smits J J T, Kroon J M, van Roosmalen J A M 2006 *J. Phys. Chem*. B **110** 19191
[24] Park N G, Schlichthorl G, Lagemaat J V D, Cheong H M, Mascarenhas A, Frank A J 1999 *J. Phys. Chem. B* **103** 3308
[25] Zeng L Y, Dai S Y, Wang K J, Pan X, Shi C W, Guo L 2004 *Chin. Phys. Lett.* **21** 835
[26] Man Gu Kang, Kwang Sun Ryu, Soon Ho Chang, Nam Gyu Park, Jin Sup Hong, Kang-Jin Kim 2004 *Bull. Korean Chem. Soc*. **25** 742
[27] B A Gregg, F Pichot, S Ferrere and C L Fields 2001 *The Journal of Physical Chemistry B*. **105** 1422-1429.
[28] Yum J H, Walter P, Huber S, Rentsch D, Geiger T, Nuesch F, De Angelis F, Gratzel M, Nazeeruddin M K 2007 J. Am. Chem. Soc. **129** 10320.
[29] Marchena M J, de Miguel G, Cohen B, Angel Organero J, Pandey S, Hayase S, Douhal J 2013 Phys. Chem. C. **117** 11906−11919.
[30] Hanna E, Susanna K, Eriksson Sandra M, Feldt Erik Gabrielsson, Peter W, Lohse, Rebecka Lindblad, Licheng Sun, Håkan Rensmo, Gerrit Boschoo, and Anders Hagfeldt 2013 *J. Phys. Chem. C*. **117** (41) 21029–21036.
[31] Yeru L, James R J, Yao H, Qing W, Shaik M Z and Michael G 2011 *J. Phys. Chem. C*. **115** (38) 18847–18855.
[32] Kawano M, Nishiyama T, Ogomi Y, Pandey S S, Ma T and Hayase S 2015 RSC Advances, RSC Adv. 5 83725–83731.
[33] Wang Z S, Cui Y, Dan-Oh Y, Kasada C, Shinpo, Hara K 2007 J. Phys. Chem. C. **111** 7224–7230.